

Supporting Information

Greazy: open-source software for automated phospholipid MS/MS identification

Michael A. Kochen¹; Matt C. Chambers¹; Jay D. Holman¹; Alexey I. Nesvizhskii²; Susan T. Weintraub³; John T. Belisle⁴; M. Nurul Islam⁴; Johannes Griss^{5,6}; David L. Tabb^{1*}

¹Department of Biomedical Informatics, Vanderbilt University, Nashville, TN 37203; ²Department of Pathology, University of Michigan, Ann Arbor, MI 48109; ³Department of Biochemistry, UT Health Science Center at San Antonio, San Antonio, TX 78229; ⁴Department of Microbiology, Immunology & Pathology, Colorado State University, Fort Collins, CO 80523; ⁵European Bioinformatics Institute (EBI), Wellcome Trust Genome Campus, Hinxton, Cambridge, U.K. CB10 1SD; ⁶Department of Dermatology, Medical University of Vienna, 1090 Vienna, Austria

* David L. Tabb, Division of Molecular Biology and Human Genetics, Stellenbosch University Faculty of Medicine and Health Sciences, Cape Town, South Africa 7550. +27 21 938 9403. dtabb@sun.ac.za

Table of Contents

Description	Page Number
GUI Configuration	S-2
Search Space Description	S-3
Tables of Predicted Fragmentation Patterns	S-4 to S-12
Search Space Characterization	S-13
NIST	S-14 to S-16
LipidSearch Comparison	S-16 to S-17
Replicates	S-18 to S-29
LipidBlast Comparison	S-29

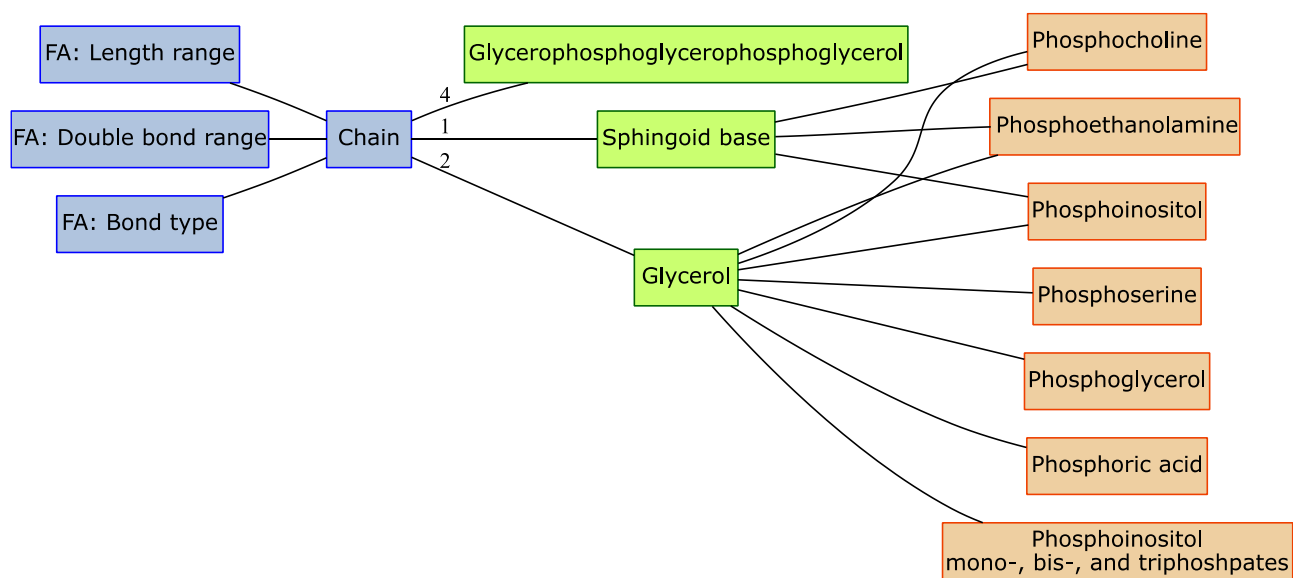


Figure S2. Greazy's lipid search space.

Supporting Text S1: *Lipid Search Space*. Each lipid is constructed by piecing it together from various backbone, head group, and fatty acyl substituents as well as the linkage types for hydrocarbon chain attachment (Figure S2).

Glycerophospholipids: Glycerophospholipids consist of a glycerol backbone, a phosphate-containing head group esterified at the *sn*-3 position of the backbone, and two fatty acyl substituents linked at the *sn*-1 and *sn*-2 positions. Several classes of lipid, defined by their head groups, can be added to the search space including glycerophosphocholines (PC), glycerophosphoethanolamines (PE), glycerophosphoinositols (PI), glycerophosphoglycerols (PG), glycerophosphoserines (PS), glycerophosphates (PA) and glycerophosphoinositol mono-, bis-, and trisphosphates (PIP). Parameters required to specify the fatty acyl substituents include ranges for the carbon chain lengths and number of double bonds for each fatty acyl group. Fatty acyl chains with an odd number of carbons can be omitted. Acyl, ether, and vinyl-ether linkages can be specified for each of the hydrocarbon chains. *Lyso*-glycerophospholipids can also be selected for inclusion.

Phosphosphingolipids: Phosphosphingolipids consist of a sphingoid backbone, a phosphate-containing head group, and a single amide linked fatty acyl group. Four sphingoid backbones, sphingosine, sphinganine, phytosphingosine, and sphingadienine can be included in the search space and a range of backbone lengths must be specified. Three classes, based on the type of head group, can be included: sphingomyelins, ceramide phosphoethanolamines, and ceramide phosphoinositols. As in the case of glycerophospholipids, a range of carbon lengths and degrees of unsaturation for the hydrocarbon chain must be specified.

Cardiolipins: Cardiolipins consist of a glycerophosphoglycerophosphoglycerol backbone and four acyl-linked carbon chains. A range of carbon chain lengths and degrees of unsaturation for each of the fatty acyl groups must be specified. Fatty acyl chains with an odd number of carbons can be omitted. *Lyso*-cardiolipins can also be included.

Table S1: Glycerophospholipids with Metal Adducts in Positive Ion Mode

	PC	PE	PS	PG	PA	PI	PIP
HG (head group) and adduct		X	X	X		X	X
loss of HG	X	X	X	X	X	X	X
loss of HG and addition of water		X	X	X	X	X	X
loss of HG and adduct	X	X	X	X	X	X	X
loss of FA1 (fatty acyl 1) as ketene	X	X	X	X	X	X	X
loss of FA1 as carboxylic acid	X	X	X	X	X	X	X
loss of HG, adduct and FA1 as ketene		X	X	X	X	X	X
loss of HG, adduct and FA1 as carboxylic acid		X	X	X	X	X	X
R1CO	X	X	X	X	X	X	X
loss of FA2 as ketene	X	X	X	X	X	X	X
loss of FA2 as carboxylic acid	X	X	X	X	X	X	X
loss of HG adduct and FA2 as ketene	X	X	X	X	X	X	X
loss of HG, adduct and FA2 as carboxylic acid		X	X	X	X	X	X
R2CO	X	X	X	X	X	X	X
loss of HGA (head group alcohol)		X	X	X		X	X
loss of HGA and FA1 as carboxylic acid	X	X	X	X		X	X
loss of HGA and FA1 as ketene		X	X	X		X	X
loss of HGA and FA2 as carboxylic acid		X	X	X		X	X
loss of HGA and FA2 as ketene		X	X	X		X	X
loss of phosphoric acid			X				
choline	X						
loss of NC3H9	X						
PO4C2H5 & adduct	X						
loss of FA1 as carboxylic acid, loss of adduct	X						
loss of FA2 as carboxylic acid, loss of adduct	X						
loss of choline & adduct, loss of FA1 as acid	X						
loss of NC3H9, loss of FA1 as acid	X						
loss of NC3H9, loss of FA2 as acid	X						
loss of HG and FA2 as acid with added D. bond	X						

Table S2: Ether (E) and Vinylether (V) Phospholipids (sn-1) with Metal Adducts in Positive Ion Mode

	PC	PE	PS	PG	PA	PI	PIP
HG (head group) and adduct		EV	EV	EV		EV	EV
loss of HG	EV	EV	EV	EV	EV	EV	EV
loss of HG and addition of water		EV	EV	EV	EV	EV	EV
loss of HG and adduct	EV	EV	EV	EV	EV	EV	EV
loss of FA2 as ketene					E		
loss of FA2 as carboxylic acid					E		
loss of HG, adduct and FA2 as carboxylic acid	EV	V	V	V	V	V	V
R2CO	EV	EV	EV	EV	EV	EV	EV
loss of HGA (head group alcohol)		EV	EV	EV		EV	EV
loss of HGA and FA1 as alcohol		V	V	V	V	V	V
loss of HGA and FA2 as carboxylic acid		E	E	E		E	E
loss of HGA and FA2 as ketene		E	E	E		E	E
loss of phosphoric acid			EV				
choline	EV						
loss of NC3H9	EV						
loss of FA2 as carboxylic acid, loss of adduct	EV						
loss of NC3H9, loss of FA2 as acid	EV						
R1 (cleavage of ether bond)	E	E	E	E	E	E	E

Table S3: Glycerophospholipid Fragments with Nonmetal Adducts in Positive Ion Mode

	PC	PE	PS	PG	PA	PI	PIP
HG (head group)	X	X	X				
loss of HG	X	X	X	X	X	X	X
loss of FA1 (fatty acyl 1) as ketene	X	X	X	X	X	X	X
loss of FA1 as carboxylic acid	X	X	X	X	X	X	X
loss of HG and FA1 as ketene	X	X	X	X	X	X	X
R1CO	X	X	X	X	X	X	X
loss of FA2 as ketene	X	X	X	X	X	X	X
loss of FA2 as carboxylic acid	X	X	X	X	X	X	X
loss of HG and FA2 as ketene	X	X	X	X	X	X	X
R2CO	X	X	X	X	X	X	X
choline	X						
loss of NC ₃ H ₉	X						

Table S4: Glycerophospholipids in Negative Ion Mode

	PC	PE	PS	PG	PA	PI
G3P-H ₂ O	X	X	X	X	X	X
G3P	X	X	X	X	X	X
H ₂ PO ₄	X	X	X	X	X	X
PO ₃	X	X	X	X	X	X
FA1 carboxylate anion	X	X	X	X	X	X
loss of FA1 as ketene	X	X	X	X	X	X
loss of FA1 as carboxylic acid	X	X	X	X	X	X
FA2 carboxylate anion	X	X	X	X	X	X
loss of FA2 as ketene	X	X	X	X	X	X
loss of FA2 as carboxylic acid	X	X	X	X	X	X
loss of HGA (head group alcohol)		X	X	X		X
loss of HGA and FA1 as carboxylic acid		X	X	X		X
loss of HGA and FA1 as ketene		X	X	X		X
loss of HGA and FA2 as carboxylic acid		X	X	X		X
loss of HGA and FA2 as ketene		X	X	X		X
head group		X	X			X
head group - H ₂ O		X				X
head group - 2*H ₂ O						X
demethylation ^a	X					
loss of C ₃ H ₁₀ N	X					
loss of C ₅ H ₁₂ N	X					
GPC-CH ₃ -H ₂ O	X					
PC-CH ₃	X					
demethylation and loss of FA1 as ketene ^a	X					
loss of C ₃ H ₁₀ N and loss of FA1 as ketene	X					
loss of C ₅ H ₁₂ N and loss of FA1 as ketene	X					
demethylation and loss of FA1 as carboxylic acid ^a	X					
loss of C ₃ H ₁₀ N and loss of FA1 as carboxylic acid	X					
loss of C ₅ H ₁₂ N and loss of FA1 as carboxylic acid	X					
demethylation and loss of FA2 as ketene ^a	X					
loss of C ₃ H ₁₀ N and loss of FA2 as ketene	X					
loss of C ₅ H ₁₂ N and loss of FA2 as ketene	X					
demethylation and loss of FA2 as carboxylic acid ^a	X					
loss of C ₃ H ₁₀ N and loss of FA2 as carboxylic acid	X					
loss of C ₅ H ₁₂ N and loss of FA2 as carboxylic acid	X					
glycerophosphoinositol						X
glycerophosphoinositol - H ₂ O						X
glycerophosphoinositol - 2*H ₂ O						X
glycerophosphoinositol - 3*H ₂ O						X
glycerophosphoglycerol				X		
glycerophosphoglycerol - H ₂ O				X		
glycerophosphoglycerol - 2*H ₂ O				X		

a. Fragment not present in demethylated precursor

Table S5: Phosphatidylinositides in Negative Ion Mode

	PIP	PIP (-2)	PIP2	PIP2 (-2)	PIP3
G3P-H2O	X	X	X	X	X
G3P					
H2PO4	X	X	X	X	X
PO3	X	X	X	X	X
FA1 carboxylate anion	X	X	X	X	X
loss of FA1 as ketene	X				
loss of FA1 as carboxylic acid	X				
FA2 carboxylate anion	X	X	X	X	X
loss of FA2 as ketene	X	X			
loss of FA2 as carboxylic acid	X				
loss of FA1 as carboxylate anion		X		X	
loss of FA2 as carboxylate anion		X		X	
loss of FA2 as ketene and PO3		X			
loss of FA2 as ketene and FA1 carboxylate anion		X			
loss of inositol phosphate	X				
loss of inositol	X				
loss of H2O	X		X		X
HO6P2	X		X	X	X
H3O7P2	X		X		X
loss of HPO3	X		X		X
loss of HPO3 & inositol			X		
loss of 2*HPO3 & inositol			X		
loss of HPO3 & inositol; addition of H2O			X		
loss of H3PO4	X		X		X
loss of 2*H3PO4					X
loss of H3PO4 & H2O			X		X
loss of inositol & H2O	X				
loss of FA1 as carboxylic acid; loss of H2O	X		X		
loss of FA2 as carboxylic acid; loss of H2O	X		X		
loss of H3PO4 & FA1 as carboxylic acid			X		X
loss of H3PO4 & FA2 as carboxylic acid			X		X
inositol phosphate		X			
inositol phosphate - H2O	X	X	X	X	X
inositol phosphate - 2*H2O	X	X	X	X	X
inositol phosphate - 3*H2O	X	X	X		X
inositol bisphosphate			X		X
inositol bisphosphate - H2O	X		X	X	X
inositol bisphosphate - 2*H2O	X		X	X	X
inositol trisphosphate + H2O			X		
inositol trisphosphate			X		X
inositol trisphosphate - H2O			X		X
inositol trisphosphate - 2*H2O			X		X
inositol tetraphosphate					X
inositol tetraphosphate - H2O					X
inositol tetraphosphate - 2*H2O					X
loss of PO3		X		X	
loss of PO3; loss of H2O				X	
bisphosphate (2-)		X			

bisphosphate - H ₂ O (2-)		X			
loss of HO ₆ P ₂				X	
loss of HO ₆ P ₂ ; loss of H ₂ O				X	
loss of PO ₃ & inositol; addition of H ₂ O				X	

Table S6: Phosphosphingolipid Fragments with Nonmetal Adducts in Positive Ion Mode

	SM	Cer-PE	Cer-PI
loss of HG	X	X	X
loss of HG and H ₂ O	X	X	X
loss of HG; addition of H ₂ O		X	X
loss of HG and fatty acid	X	X	X
loss of HG and fatty acid; addition of H ₂ O	X	X	
fatty acid + NC ₂ H ₃	X	X	X
fatty acid + NH ₃	X	X	X
HG	X	X	
loss of NC ₃ H ₉	X		
HGA	X		
loss of HGA		X	
loss of H ₂ O			X
loss of 2*H ₂ O			X

Table S7: Phosphosphingolipid Fragments with Metal Adducts in Positive Ion Mode

	SM	Cer-PE	Cer-PI
loss of HG	X	X	X
loss of HG and adduct	X	X	X
loss of HG , adduct, and H ₂ O	X	X	X
loss of HG and H ₂ O	X	X	
loss of HG and CH ₂ O	X	X	X
loss of HG, adduct, and FA	X	X	X
loss of HG and FA; addition of H ₂ O	X	X	
FA + NC ₂ H ₃	X	X	X
FA + NH ₃	X	X	X
FA + NH ₃ and adduct	X	X	
HG	X	X	
loss of NC ₃ H ₉	X		
HGA	X		
PO ₄ C ₂ H ₅ and adduct	X		
loss of HG; addition of water		X	X
loss of HGA		X	X
loss of HGA and H ₂ O			X
HG and adduct			X
HG and adduct minus H ₂ O			X
loss of H ₂ O			X

Table S8: Phosphosphingolipid Fragments in Negative Ion Mode

SL negative mode	SM	Cer-PE	Cer-PI
loss of methyl group ^a	X		
loss of C3H10N	X		
loss of HGA and adduct	X		
loss of HGA		X	X
HG		X	X
HG – H ₂ O		X	X
HG – 2H ₂ O			X

Table S9: Cardiolipin Fragments in Positive Ion Mode

protonated, + Alkali Metal, - H + 2Alkali Metal	CL - 2H + 3Alkali Metal
loss of FA1, FA2, & glycerol	loss of FA1 as carboxylic acid
loss of FA1, FA2, glycerol, & H ₂ O	loss of FA2 as carboxylic acid
loss of FA3, FA4, & glycerol	loss of FA3 as carboxylic acid
loss of FA3, FA4, glycerol, & H ₂ O	loss of FA4 as carboxylic acid
loss of FA1, FA2, glycerol & glycerol-1,3-diphosphate ^b	loss of FA1 & FA3 as carboxylic acids
loss of FA1, FA2, FA3, glycerol & glycerol-1,3-diphosphate ^b	loss of FA1 & FA2 as carboxylic acids
FA3 cation	loss of FA3 & FA4 as carboxylic acids
FA4 cation	loss of FA1, FA2, and glycerol
loss of FA3, FA4, glycerol & glycerol-1,3-diphosphate ^b	loss of FA1, FA2, glycerol, and FA3 as a carboxylic acid
loss of FA3, FA4, FA1, glycerol & glycerol-1,3-diphosphate ^b	loss of FA1, FA2, glycerol, and FA3 as an alkali salt
FA1 cation	loss of FA1, FA2, glycerol, and FA4 as a carboxylic acid
FA2 cation	loss of FA1, FA2, glycerol, and FA4 as an alkali salt
	loss of FA3, FA4, and glycerol
	loss of FA3, FA4, glycerol, and FA1 as a carboxylic acid
	loss of FA3, FA4, glycerol, and FA1 as an alkali salt
	loss of FA3, FA4, glycerol, and FA2 as a carboxylic acid
	loss of FA3, FA4, glycerol, and FA2 as an alkali salt
	loss of FA1, FA2, and sodiated glycerophosphatidic acid
	loss of FA1, FA2, sodiated glycerophosphatidic acid, and FA3 as a carboxylic acid
	loss of FA1, FA2, and phosphoglycerophosphate

b. Loss of metal adduct if present (sodium, di-sodium, etc.)

Table S10: Cardiolipin Fragments in Negative Ion Mode – Deprotonated

G3P-H ₂ O
G3P
H ₂ PO ₄
PO ₃
FA1 carboxylate anion
FA2 carboxylate anion
FA3 carboxylate anion
FA4 carboxylate anion
loss of FA1 as carboxylic acid
loss of FA2 as carboxylic acid
loss of FA3 as carboxylic acid
loss of FA4 as carboxylic acid
loss of FA1, FA2 & glycerol
loss of FA1, FA2, FA3 as carboxylic acid & glycerol
loss of FA1, FA2, FA4 as carboxylic acid & glycerol
loss of FA1, FA2, FA3 as ketene & glycerol
loss of FA1, FA2, FA4 as ketene & glycerol
loss of FA1, FA2 & phosphoglycerol
loss of FA1, FA2, FA3 as carboxylic acid & glycerophosphoglycerol
loss of FA1, FA2, FA4 as carboxylic acid & glycerophosphoglycerol
loss of FA1, FA2, FA3 as ketene & glycerophosphoglycerol
loss of FA1, FA2, FA4 as ketene & glycerophosphoglycerol
loss of FA1, FA2, phosphoglycerol & FA3 as a carboxylic acid
loss of FA1, FA2, phosphoglycerol & FA4 as a carboxylic acid
loss of FA1, FA2, phosphoglycerol & FA3 as a ketene
loss of FA1, FA2, phosphoglycerol & FA4 as a ketene
loss of FA1, FA2 & glycerophosphoglycerol
loss of FA3, FA4 & glycerol
loss of FA3, FA4, FA1 as carboxylic acid & glycerol
loss of FA3, FA4, FA2 as carboxylic acid & glycerol
loss of FA3, FA4, FA1 as ketene & glycerol
loss of FA3, FA4, FA2 as ketene & glycerol
loss of FA3, FA4 & phosphoglycerol
loss of FA3, FA4, FA1 as carboxylic acid & glycerophosphoglycerol
loss of FA3, FA4, FA2 as carboxylic acid & glycerophosphoglycerol
loss of FA3, FA4, FA1 as ketene & glycerophosphoglycerol
loss of FA3, FA4, FA2 as ketene & glycerophosphoglycerol
loss of FA3, FA4, phosphoglycerol & FA1 as a carboxylic acid
loss of FA3, FA4, phosphoglycerol & FA2 as a carboxylic acid
loss of FA3, FA4, phosphoglycerol & FA1 as a ketene
loss of FA3, FA4, phosphoglycerol & FA2 as a ketene
loss of FA3, FA4 & glycerophosphoglycerol

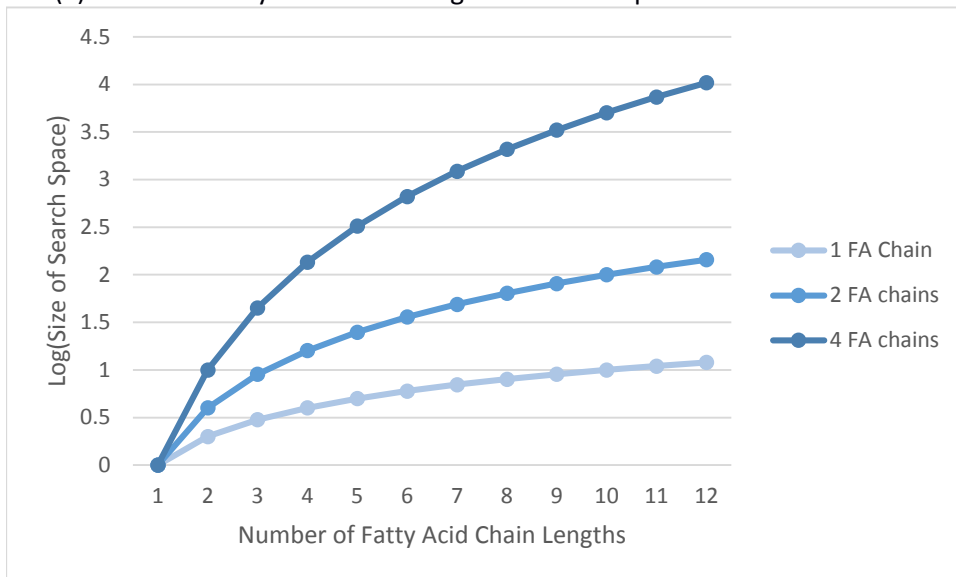
Table S11: Cardiolipin Fragments in Negative Ion Mode – Doubly Deprotonated

G3P-H ₂ O
G3P
H ₂ PO ₄
PO ₃
loss of FA1 carboxylic anion
loss of FA2 carboxylic anion
loss of FA3 carboxylic anion
loss of FA4 carboxylic anion
FA1 carboxylate anion
FA2 carboxylate anion
FA3 carboxylate anion
FA4 carboxylate anion
loss of FA2 as ketene
loss of FA4 as ketene
loss of FA1, FA2 & phosphoglycerol
loss of FA1, FA2, phosphoglycerol & FA3 as a carboxylic acid
loss of FA1, FA2, phosphoglycerol & FA4 as a carboxylic acid
loss of FA1, FA2, phosphoglycerol & FA3 as a ketene
loss of FA1, FA2, phosphoglycerol & FA4 as a ketene
loss of FA1, FA2 & glycerophosphoglycerol
loss of FA1, FA2, FA3 as carboxylic acid & glycerophosphoglycerol
loss of FA1, FA2, FA4 as carboxylic acid & glycerophosphoglycerol
loss of FA1, FA2, FA3 as ketene & glycerophosphoglycerol
loss of FA1, FA2, FA4 as ketene & glycerophosphoglycerol
loss of FA3, FA4 & phosphoglycerol
loss of FA3, FA4, phosphoglycerol & FA1 as a carboxylic acid
loss of FA3, FA4, phosphoglycerol & FA2 as a carboxylic acid
loss of FA3, FA4, phosphoglycerol & FA1 as a ketene
loss of FA3, FA4, phosphoglycerol & FA2 as a ketene
loss of FA3, FA4 & glycerophosphoglycerol
loss of FA3, FA4, FA1 as carboxylic acid & glycerophosphoglycerol
loss of FA3, FA4, FA2 as carboxylic acid & glycerophosphoglycerol
loss of FA3, FA4, FA1 as ketene & glycerophosphoglycerol
loss of FA3, FA4, FA2 as ketene & glycerophosphoglycerol

Table S12: Cardiolipin Fragments in Negative Ion Mode – Doubly Deprotonated plus Alkali Metal

CL - 2H + Alkali Metal
loss of FA1 as a carboxylic acid
loss of FA2 as a carboxylic acid
loss of FA3 as a carboxylic acid
loss of FA4 as a carboxylic acid
loss of FA1 as a ketene
loss of FA2 as a ketene
loss of FA3 as a ketene
loss of FA4 as a ketene
loss of FA1 as an alkali salt
loss of FA2 as an alkali salt
loss of FA3 as an alkali salt
loss of FA4 as an alkali salt
loss of FA1, FA2 & glycerol
loss of FA1, FA2 & glycerol and FA3 as a carboxylic acid
loss of FA1, FA2 & glycerol and FA3 as a ketene
loss of FA1, FA2 & glycerol and FA3 as an alkali salt
loss of FA1, FA2 & glycerol and FA4 as a carboxylic acid
loss of FA1, FA2 & glycerol and FA4 as a ketene
loss of FA1, FA2 & glycerol and FA4 as an alkali salt
loss of FA3, FA4 & glycerol
loss of FA3, FA4 & glycerol and FA1 as a carboxylic acid
loss of FA3, FA4 & glycerol and FA1 as a ketene
loss of FA3, FA4 & glycerol and FA1 as an alkali salt
loss of FA3, FA4 & glycerol and FA2 as a carboxylic acid
loss of FA3, FA4 & glycerol and FA2 as a ketene
loss of FA3, FA4 & glycerol and FA2 as an alkali salt
loss of FA1, FA2 & glycerophosphoglycerol
loss of FA1, FA2 & glycerophosphoglycerol and FA3 as an alkali salt
loss of FA1, FA2 & glycerophosphoglycerol and FA4 as an alkali salt
loss of FA3, FA4 & glycerophosphoglycerol
loss of FA3, FA4 & glycerophosphoglycerol and FA1 as an alkali salt
loss of FA3, FA4 & glycerophosphoglycerol and FA2 as an alkali salt
loss of FA1, FA2, and alkalated glycerophosphatidic acid
loss of FA3, FA4, and alkalated glycerophosphatidic acid

(a) Effect of Fatty Acid Chain Length on Search Space Size



(b) Effect of Chain Length and Double Bond Content on Search Space Size

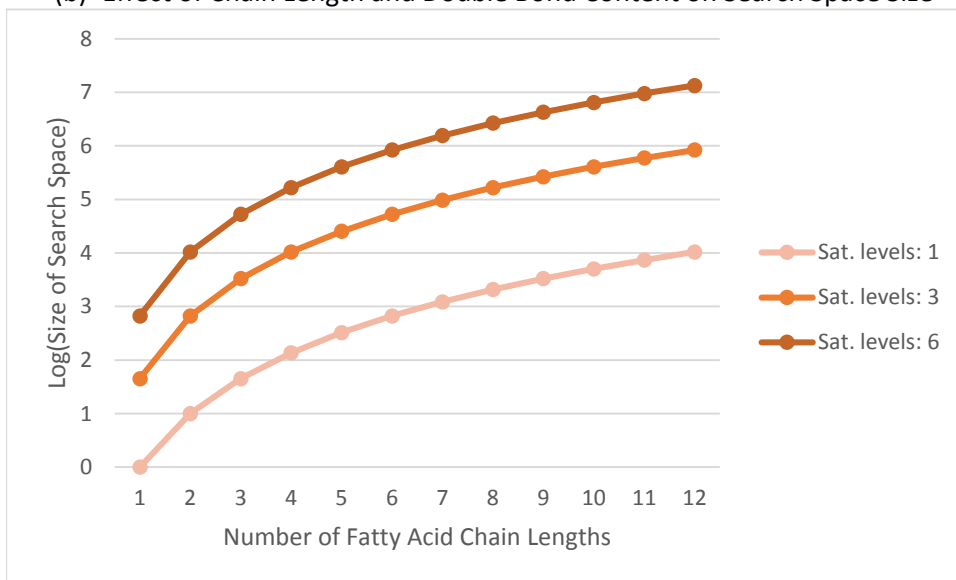


Figure S3. The search space grows rapidly as the number of possible fatty acid chain lengths increases, particularly for lipids with a greater number of fatty acid substituents (a). The number of possible saturation levels similarly affects the size of the search space and when combined can make the search space infeasibly large (b).

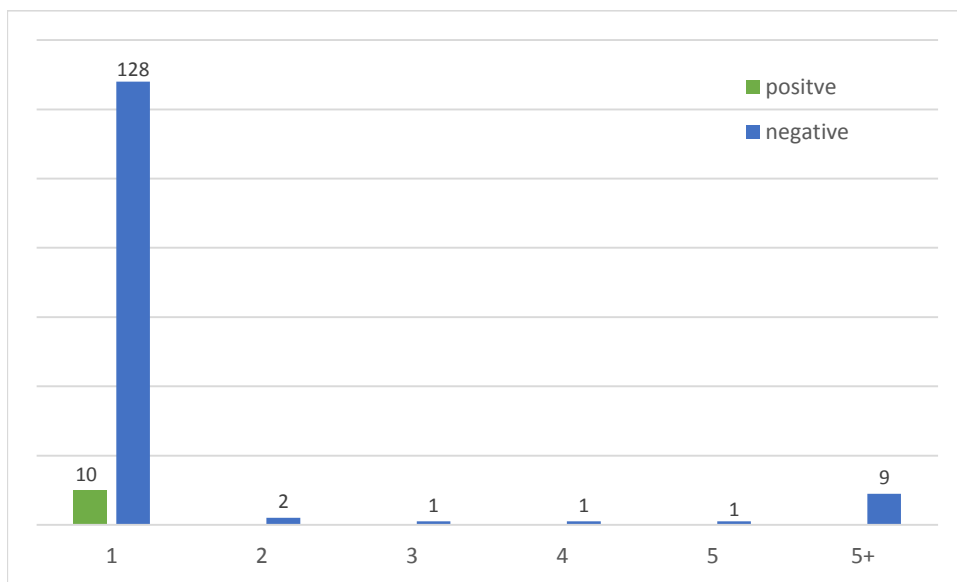


Figure S4. Correct match ranks for spectra in the NIST library, filtered at 5% FDR, whose identity falls within the search space.

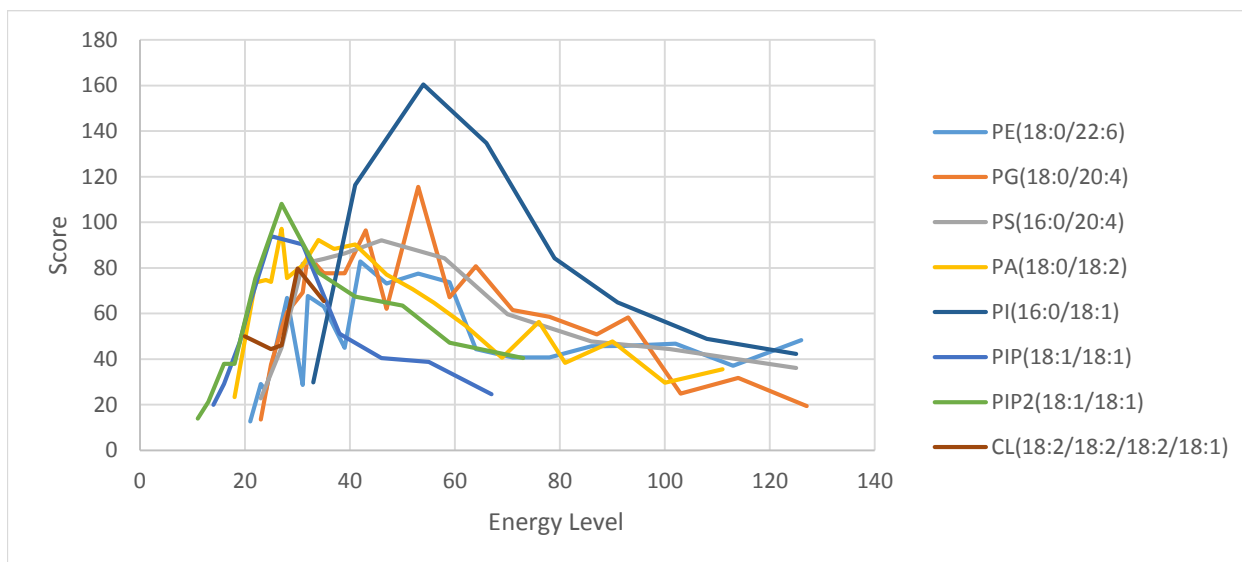


Figure S5. Score vs collision energy for examples of several lipid classes in negative ion mode. In each case the highest score was attained within the first half of the given energy range.

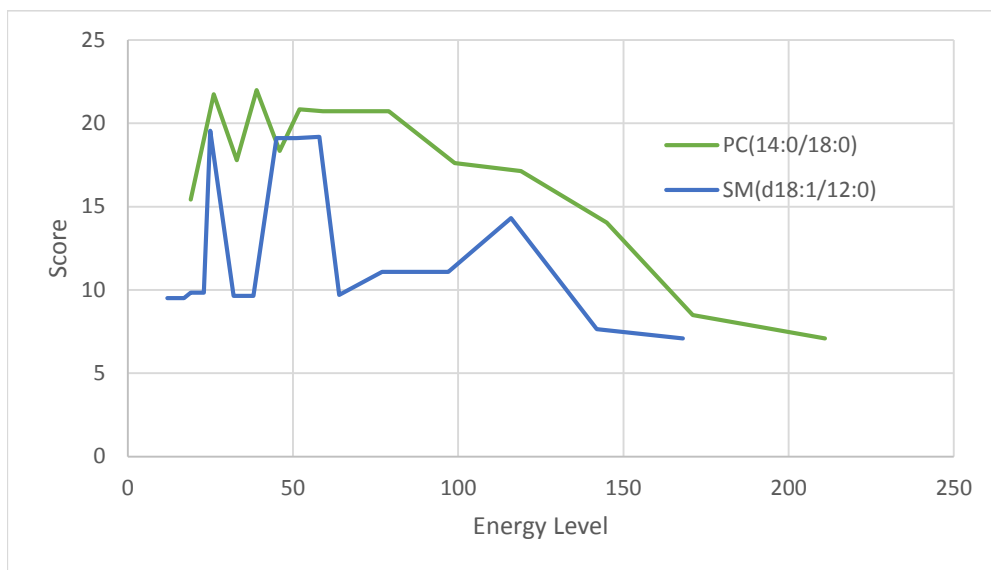


Figure S6. Score vs collision energy for a PC and an SM in positive ion mode. In both cases the high score was attained at the low end of the energy range.

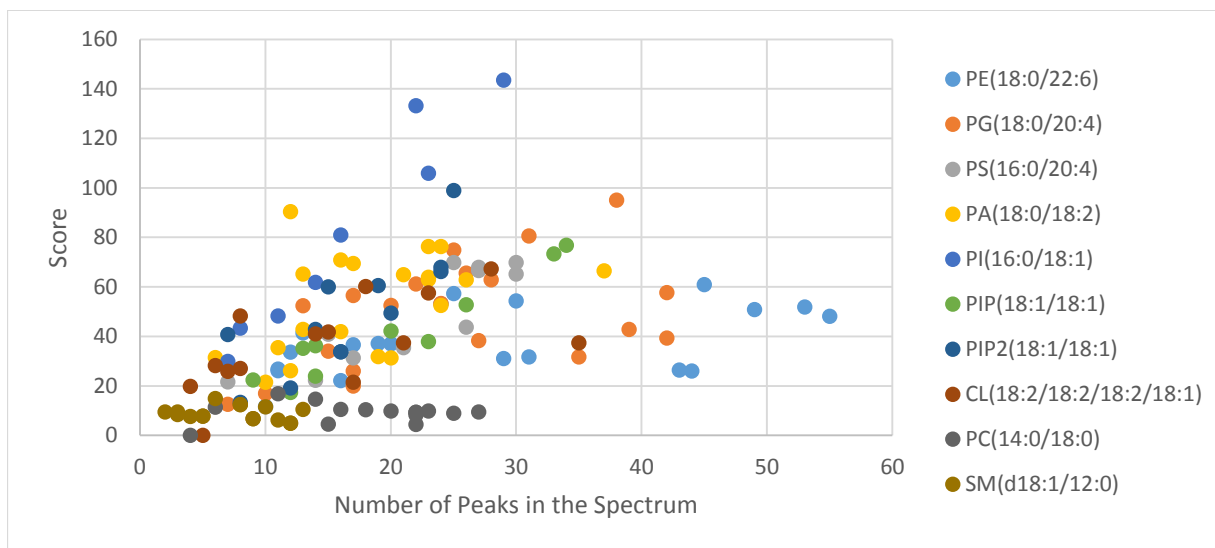


Figure S7. Score vs spectrum peak count. For those lipids run in negative ion mode the score obtained with Greazy generally rises with the number of peaks in the spectrum. For those run in positive mode the score obtained is flat regardless of the number of peaks in the spectrum.

Supporting Text S2: *Greazy at Various Energy Levels*. Many of the phospholipids within the NIST metabolomics library were measured at various collision energies in a Thermo Finnigan LTQ Orbitrap Elite by ion trap collision-induced dissociation (CID) and higher-energy collisional dissociation (HCD), allowing us to test Greazy under different energy levels. Under HCD conditions we looked at several classes of glycerophospholipids and a cardiolipin species in negative ion mode (Figure S5) and considered a PC and an SM in positive ion mode (Figure S6). In negative ion mode the collision energy ranged from 11 to 127 (normalized), and every lipid surveyed in this mode had its best score in the lower half of this range. In positive mode both PCs and SMs scored poorly at all energy levels. By contrast, spectra for these species within the NIST library that were generated by ion trap CID produced much higher scores, recommending a different experimental setup for identification of PCs and SMs in positive mode. We also found that higher scores are obtained when comparing against spectra with higher peak counts; this relationship is illustrated in Figure S7.

It should be noted that the fragmentation models in Greazy do not explicitly account for collision energies or other collision conditions such as gas pressure or cell type. Instead we have specified only the expected m/z values for each lipid, taking into account adducts and polarity. We then used a probabilistic approach to scoring (see Methods) that we expect will implicitly account for variations in peak count and ion intensity that arise from differing experimental conditions.

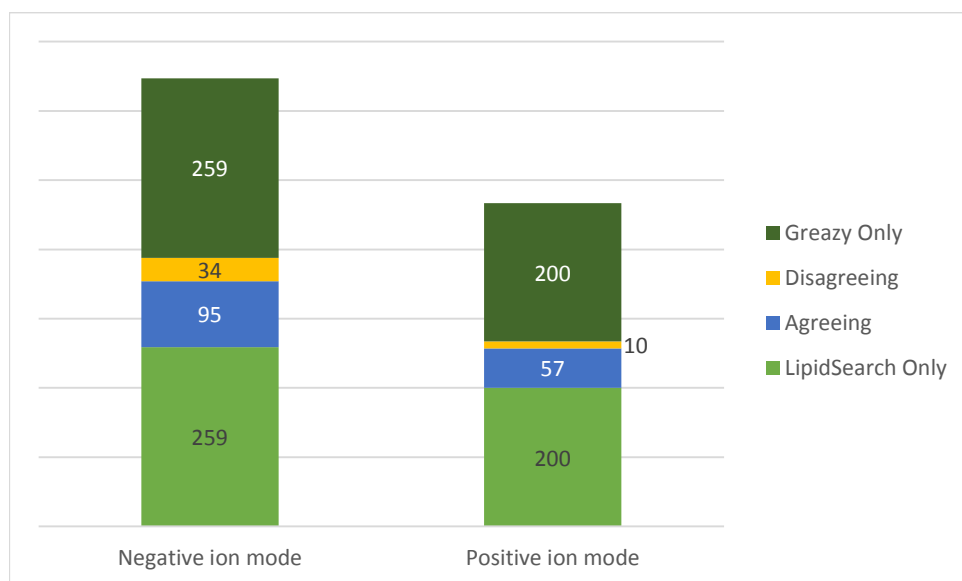
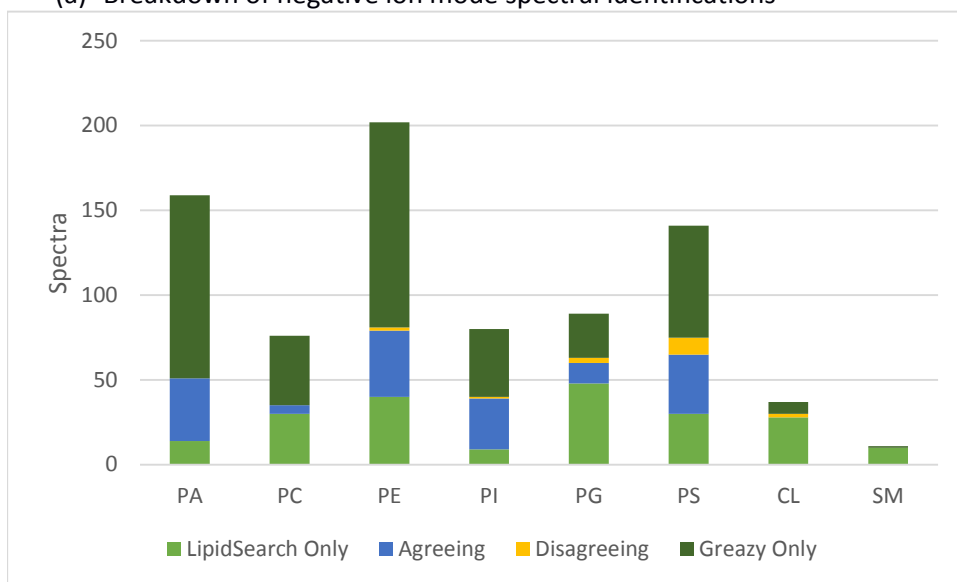


Figure S8. Comparison of Greazy/LipidLama and LipidSearch at the spectrum level when the same number of lipids is retained.

(a) Breakdown of negative ion mode spectral identifications



(b) Breakdown of positive ion mode spectral identifications

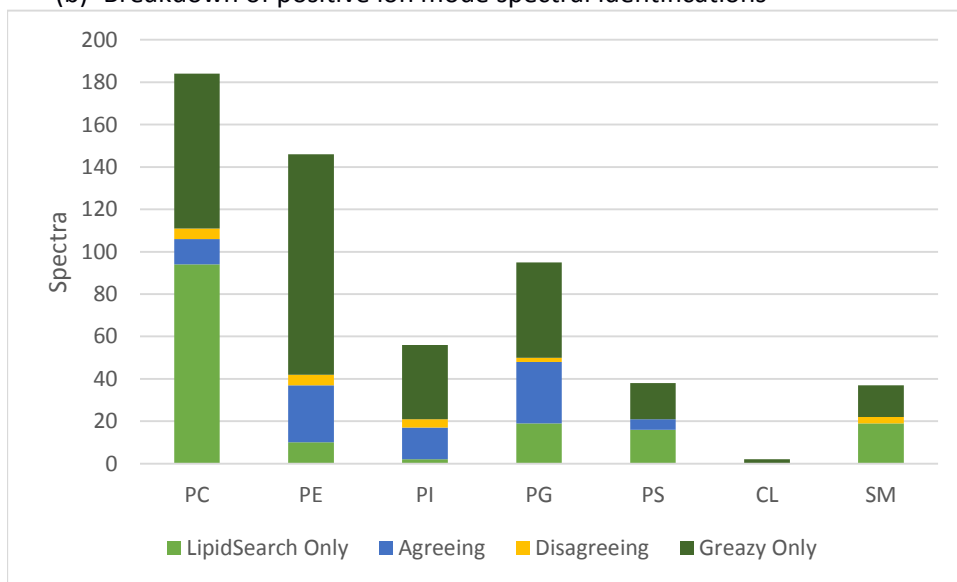
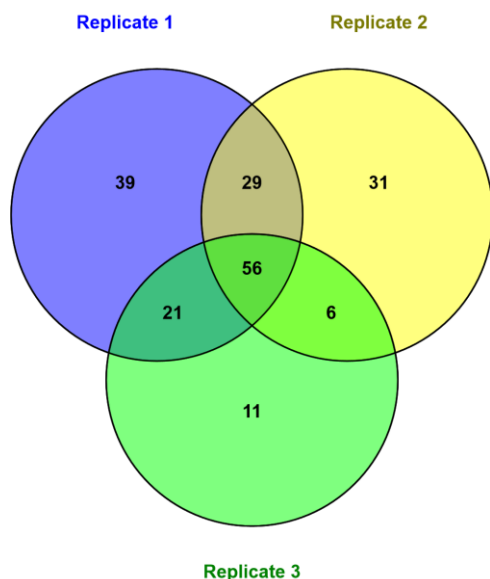


Figure S9. Overlap of class specific spectral identifications made by LipidSearch and Greazy in negative (a) and positive (b) ion mode. Greazy's results were filtered by LipidLama at a 90% confidence level.

(a) Day 7 alveolar type 2 epithelial cells



(b) Day 28 alveolar type 2 epithelial cells

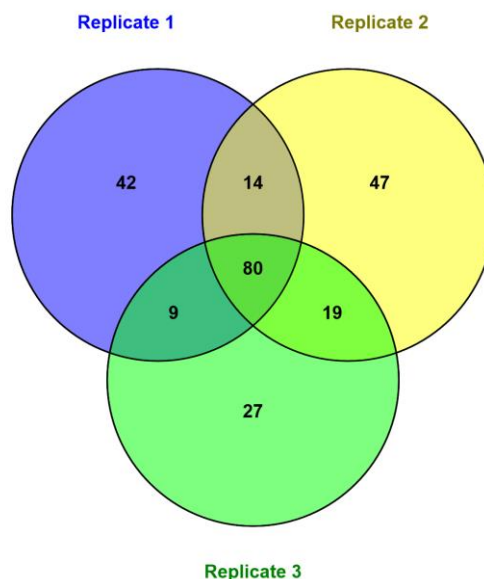


Figure S10. A Greazy search of three replicates each of day 7 (a) and day 28 (b) alveolar type 2 epithelial cells at 10% FDR. 193 and 238 distinct lipids were identified among all replicates in the day 7 and day 28 replicates respectively.

Supporting Text S3: Alveolar Type 2 Epithelial Cells. The alveolar type 2 epithelial cell data consisted of three biological replicates each of the day-7 and day-28 alveolar type 2 epithelial cells (see methods). The search space included the glycerophospholipids PE, PI, PG, PS and their lyso- counterparts with fatty acyl chains of 12-24 carbons and 0-6 double bonds. The search was made in negative mode and included only singly deprotonated precursors. A 20 ppm mass accuracy tolerance was used for both precursor and fragment ions. LipidLama was applied at a 10% estimated FDR.

For the day-7 cells there were 145, 122, and 94 distinct lipids reported in replicates 1-3 respectively. 193 distinct lipids were found among all replicates, with 56 (29%) of them present in all three (Figure S10a). Among these 56 lipids were PEs, PGs, and a single PS (Supporting Table S13). The day 28 cells showed 145, 160, and 135 distinct lipids in replicates 1-3, and a total of 238 distinct lipids. 80 (34%) of these lipids were present in all three replicates (Figure S10b) with representatives from all four classes in the search space. Most of the lipids found in all replicates of either group have fatty acyl chain lengths with an even number of carbons and double bond configurations that commonly exist in mammalian lipids (16:0, 20:4, 22:6, etc.). Three scored spectra, representing high, medium, and low scoring lipids from one replicate of the day-7 cells are given in figure S11. The low scoring PG(20:4/22:5) may indicate that a stricter FDR level is appropriate for this particular lipid class. If one wishes to weed out structurally unlikely lipids, such as those with two polyunsaturated fatty acyls, or an odd number of carbons, it must be done when defining the search space. Greazy gives no weight to such characteristics. There were 81 and 116 lipids in the day-7 and day-28 groups respectively that were found in only one replicate. This suggests a degree of variability among biological replicates that is reminiscent of that seen in proteomics (see Tabb et al., *J. Proteome Res.* 2010, 9, 761–776). A range of FDR levels were examined for the day 28 replicates (Supporting Figure S12). The percentage of lipids found in the intersection of the replicates was highest in a range of 8-14% FDR.

Table S13. Lipids present in all three replicates of day 7 and day 28 alveolar type 2 epithelial cells.

Day 7			Day 28			
PE(14:0/16:0)	PG(13:3/16:0)	PS(18:0/22:6)	PE(14:0/16:0)	PG(13:2/16:1)	PI(16:0/20:5)	PS(16:0/20:4)
PE(14:0/20:4)	PG(15:0/16:0)		PE(14:0/16:1)	PG(13:2/23:3)	PI(18:0/20:3)	PS(16:0/21:4)
PE(14:0/22:6)	PG(16:0/16:0)		PE(14:0/18:2)	PG(13:3/16:0)	PI(18:0/20:4)	PS(17:2/23:3)
PE(16:0/0:0)	PG(16:0/16:1)		PE(14:0/20:4)	PG(14:0/16:0)	PI(18:0/20:5)	PS(18:0/20:3)
PE(16:0/16:0)	PG(16:0/18:1)		PE(14:0/22:6)	PG(15:0/16:1)	PI(18:0/22:5)	PS(18:0/20:4)
PE(16:0/16:1)	PG(16:0/18:2)		PE(14:1/18:0)	PG(15:0/18:2)	PI(18:1/20:4)	PS(18:0/22:5)
PE(16:0/17:1)	PG(16:0/18:3)		PE(15:0/18:0)	PG(15:1/23:3)		PS(18:1/20:4)
PE(16:0/18:0)	PG(16:0/20:3)		PE(16:0/0:0)	PG(15:3/19:0)		PS(20:4/24:1)
PE(16:0/18:1)	PG(16:0/20:4)		PE(16:0/16:0)	PG(16:0/0:0)		
PE(16:0/20:1)	PG(16:0/22:6)		PE(16:0/16:1)	PG(16:0/16:0)		
PE(16:0/20:4)	PG(16:1/22:6)		PE(16:0/18:0)	PG(16:0/16:1)		
PE(16:0/20:5)	PG(18:0/22:6)		PE(16:0/18:1)	PG(16:0/16:2)		
PE(16:0/22:5)	PG(18:1/18:2)		PE(16:0/18:2)	PG(16:0/17:1)		
PE(16:0/22:6)	PG(18:1/22:6)		PE(16:0/20:3)	PG(16:0/18:0)		
PE(16:1/18:1)	PG(18:2/20:4)		PE(16:0/20:4)	PG(16:0/18:1)		
PE(16:1/18:2)	PG(18:2/22:5)		PE(16:0/20:5)	PG(16:0/18:2)		
PE(16:1/20:4)	PG(18:2/22:6)		PE(16:0/22:4)	PG(16:0/20:3)		
PE(16:1/22:6)	PG(20:4/22:6)		PE(16:0/22:5)	PG(16:0/20:4)		
PE(17:0/20:4)	PG(20:5/22:6)		PE(16:0/22:6)	PG(16:0/20:5)		
PE(18:0/18:1)	PG(22:5/22:6)		PE(16:1/16:1)	PG(16:0/22:5)		
PE(18:0/18:2)			PE(16:1/18:0)	PG(16:0/22:6)		
PE(18:0/20:3)			PE(16:1/18:1)	PG(16:0/23:6)		
PE(18:0/20:4)			PE(16:1/18:2)	PG(16:0/24:5)		
PE(18:0/22:4)			PE(16:1/20:1)	PG(16:1/17:1)		
PE(18:0/22:5)			PE(16:1/20:2)	PG(16:1/18:0)		
PE(18:0/22:6)			PE(16:1/20:4)	PG(16:1/18:1)		
PE(18:1/18:2)			PE(16:1/20:5)	PG(16:1/18:2)		
PE(18:1/20:3)			PE(16:1/22:0)	PG(16:1/20:1)		
PE(18:1/22:6)			PE(16:1/22:6)	PG(16:1/20:4)		
PE(18:2/20:4)			PE(16:1/24:0)	PG(16:1/20:5)		
PE(20:4/22:0)			PE(17:0/18:1)	PG(16:1/22:6)		
PE(20:4/22:1)			PE(17:0/20:4)	PG(17:0/18:1)		
PE(20:4/24:0)			PE(18:0/0:0)	PG(17:0/18:2)		
PE(20:4/24:1)			PE(18:0/18:0)	PG(17:1/20:4)		
PE(22:6/0:0)			PE(18:0/18:1)	PG(17:2/23:3)		
			PE(18:0/18:2)	PG(17:3/24:3)		
			PE(18:0/20:2)	PG(18:0/18:2)		
			PE(18:0/20:3)	PG(18:0/20:4)		
			PE(18:0/20:4)	PG(18:0/20:5)		
			PE(18:0/20:5)	PG(18:0/22:5)		
			PE(18:0/22:4)	PG(18:0/22:6)		
			PE(18:0/22:5)	PG(18:1/18:2)		
			PE(18:0/22:6)	PG(18:1/20:4)		
			PE(18:1/18:1)	PG(18:1/22:5)		
			PE(18:1/18:2)	PG(18:1/22:6)		
			PE(18:1/20:1)	PG(18:2/20:4)		
			PE(18:1/20:4)	PG(18:2/20:5)		
			PE(18:1/20:5)	PG(18:2/22:5)		
			PE(18:1/22:6)	PG(18:2/22:6)		

			PE(18:1/24:0)	PG(18:2/23:5)		
			PE(18:2/20:4)	PG(18:3/22:6)		
			PE(18:2/24:0)	PG(20:3/23:5)		
			PE(19:0/20:4)	PG(20:4/21:5)		
			PE(20:0/20:4)	PG(20:4/22:5)		
			PE(20:3/22:0)	PG(20:4/22:6)		
			PE(20:4/0:0)	PG(20:5/22:5)		
			PE(20:4/22:0)	PG(20:5/22:6)		
			PE(20:4/22:1)	PG(22:5/22:6)		
			PE(20:4/23:0)	PG(22:6/22:6)		
			PE(20:4/24:0)			
			PE(20:4/24:1)			
			PE(22:6/0:0)			

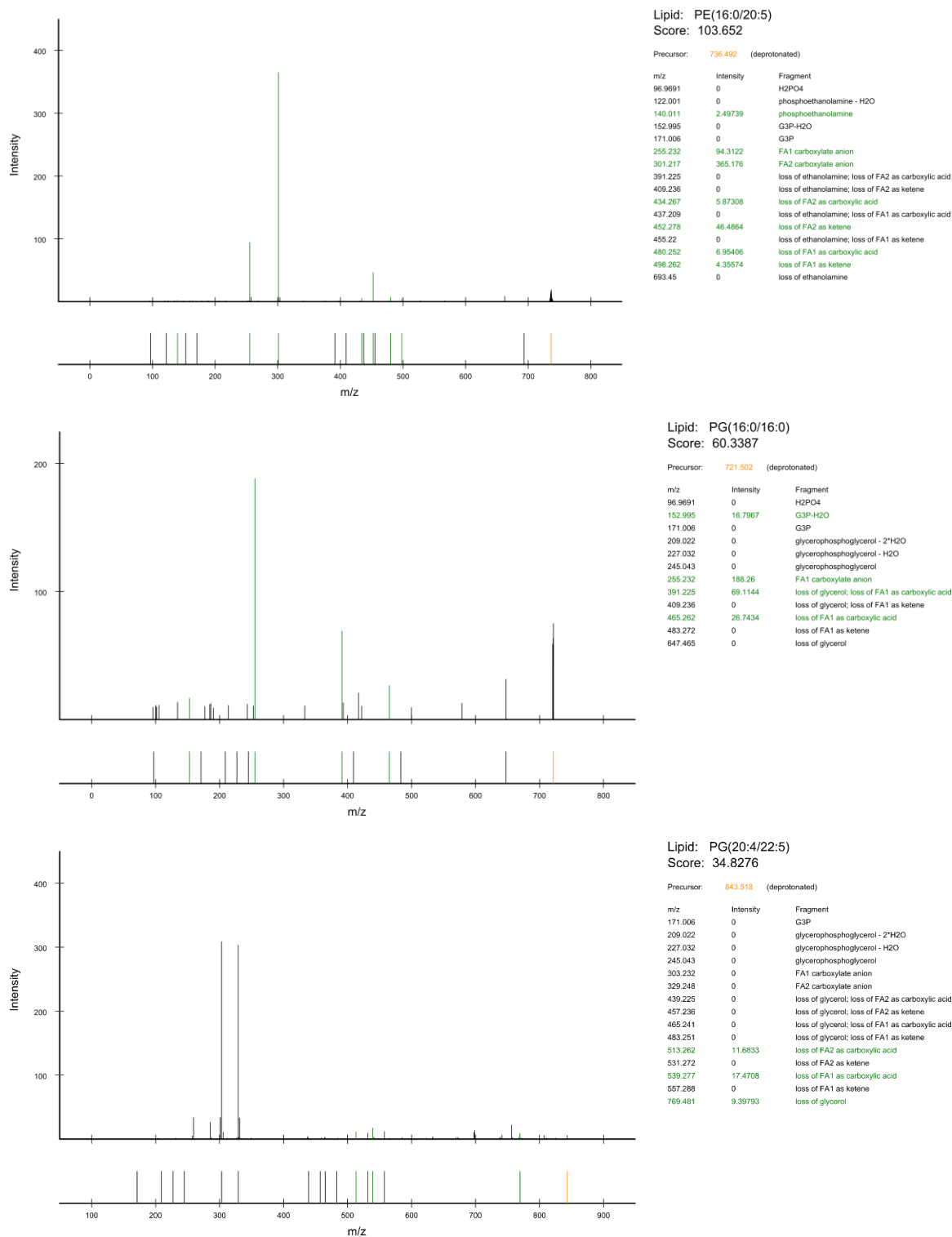


Figure S11. Three examples of spectra from one replicate of the day 7 alveolar type 2 epithelial cells.

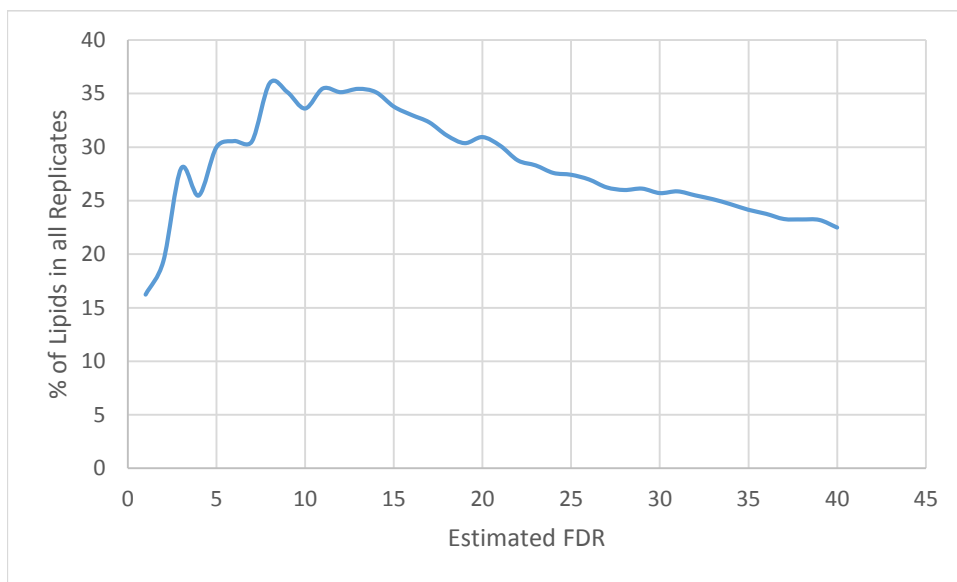


Figure S12. LipidLama FDR setting vs. the percentage of lipids found in all day 28 alveolar type 2 epithelial cells.

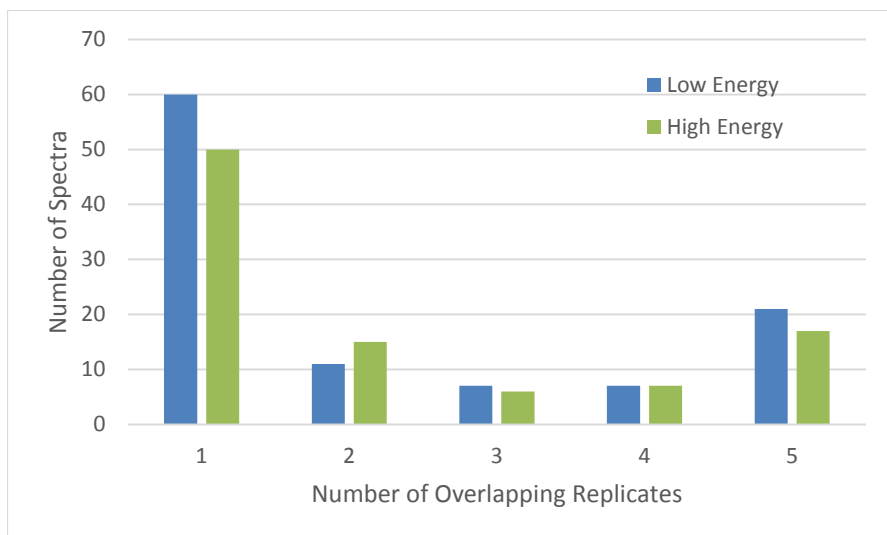


Figure S13. Lipid identification distributions for the human plasma replicates. Each identified lipid falls into at least one and as many 5 replicates for each set.

Table S14. Lipids present in low energy technical replicates.

5 count	4 count	3 count	2 count	1 count
PC(0:0/16:0)	PC(0:0/18:0)	PC(16:0/22:5)	PA(O-18:0/18:1)	PA(18:1/24:1)
PC(16:0/18:1)	PC(0:0/18:2)	PC(18:0/18:1)	PC(16:0/20:2)	PA(22:1/20:2)
PC(16:0/18:2)	PC(18:0/20:4)	PE(0:0/16:0)	PC(18:1/20:4)	PA(24:1/18:2)
PC(16:0/20:3)	PE(0:0/18:1)	PE(16:0/22:6)	PE(O-16:1/22:6)	PA(O-20:0/18:1)
PC(16:0/20:4)	PE(0:0/18:2)	PE(18:1/18:2)	PE(O-18:1/18:2)	PA(O-24:1/16:0)
PC(16:0/20:5)	PE(16:0/18:2)	PE(O-16:1/18:2)	PE(P-18:1/18:2)	PA(P-24:1/14:0)
PC(18:0/18:2)	PI(16:0/18:1)	PS(16:0/22:3)	PI(16:0/20:3)	PC(0:0/16:1)
PC(18:0/20:3)			PI(18:1/18:2)	PC(0:0/18:1)
PC(18:1/18:2)			PS(18:0/20:3)	PC(0:0/20:4)
PE(0:0/18:0)			PS(18:0/22:3)	PC(16:0/16:1)
PE(18:0/18:2)			PS(P-24:1/20:6)	PC(16:0/18:3)
PE(18:0/20:4)				PC(16:0/22:4)
PE(O-16:1/20:4)				PC(16:0/22:6)
PE(O-18:1/20:4)				PC(16:1/18:1)
PE(P-18:1/20:4)				PC(16:1/18:2)
PI(16:0/18:2)				PC(18:0/22:5)
PI(16:0/20:4)				PC(18:1/18:1)
PI(18:0/18:2)				PC(P-16:1/22:5)
PI(18:0/20:3)				PC(P-18:1/20:5)
PI(18:0/20:4)				PE(16:0/18:1)
PI(18:1/20:4)				PE(16:0/20:4)
				PE(18:1/20:3)
				PE(18:1/20:4)
				PE(O-18:1/18:1)
				PE(O-18:1/20:5)
				PG(16:0/22:4)
				PG(18:0/18:1)
				PG(O-20:1/16:0)
				PG(O-20:1/18:0)
				PG(O-20:1/22:0)
				PG(O-20:1/24:0)
				PG(O-22:0/16:2)
				PG(O-22:1/16:0)
				PG(O-22:1/16:1)
				PG(O-22:1/18:1)
				PG(O-24:0/18:2)
				PG(O-24:0/20:1)
				PG(O-24:1/20:1)
				PG(P-20:1/16:0)
				PG(P-20:1/24:0)
				PI(18:0/18:1)
				PS(16:0/22:1)
				PS(16:0/22:2)
				PS(16:0/24:5)
				PS(18:0/20:1)
				PS(18:1/22:3)
				PS(20:0/18:2)

				PS(22:1/22:6)
				PS(24:1/20:6)
				PS(O-14:0/22:2)
				PS(O-18:1/20:3)
				PS(O-20:0/16:0)
				PS(O-24:0/14:4)
				PS(P-18:1/24:4)
				PS(P-18:1/24:6)
				PS(P-20:1/16:0)
				PS(P-20:1/18:1)
				PS(P-20:1/20:4)
				PS(P-20:1/24:6)
				PS(P-24:1/20:5)

Table S15. Lipids present in high energy technical replicates.

5 count	4 count	3 count	2 count	1 count
PC(16:0/18:1)	PC(0:0/16:0)	PC(18:0/20:4)	PC(0:0/18:1)	PA(O-20:1/16:0)
PC(16:0/18:2)	PC(0:0/18:0)	PE(O-16:1/20:4)	PC(0:0/18:2)	PC(14:0/18:1)
PC(16:0/20:3)	PC(16:0/22:5)	PE(P-18:1/18:2)	PC(16:0/16:0)	PC(14:0/18:2)
PC(16:0/20:4)	PC(18:1/18:2)	PI(18:0/20:3)	PC(16:0/22:6)	PC(16:0/16:1)
PC(18:0/18:1)	PE(0:0/16:0)	PI(18:1/18:2)	PE(16:0/20:4)	PC(16:0/20:2)
PC(18:0/18:2)	PE(0:0/18:0)	PI(18:1/20:4)	PE(16:0/22:6)	PC(16:1/18:1)
PC(18:0/20:3)	PE(16:0/18:2)		PE(18:1/18:2)	PC(16:1/18:2)
PE(18:0/18:2)			PE(O-16:1/18:2)	PC(16:1/20:3)
PE(18:0/20:4)			PE(O-16:1/20:3)	PC(18:0/22:5)
PE(O-18:1/20:4)			PE(O-16:1/22:6)	PC(18:1/20:4)
PE(P-18:1/20:4)			PE(O-18:1/18:2)	PC(18:1/20:5)
PI(16:0/18:1)			PG(O-20:1/16:0)	PE(0:0/18:2)
PI(16:0/18:2)			PG(O-20:1/22:0)	PE(0:0/20:4)
PI(16:0/20:4)			PG(O-22:1/16:1)	PE(18:0/18:1)
PI(18:0/18:1)			PS(P-20:1/18:1)	PE(18:0/20:5)
PI(18:0/18:2)				PE(18:0/22:6)
PI(18:0/20:4)				PE(18:1/18:1)
				PE(18:1/20:3)
				PE(18:1/20:4)
				PE(O-12:1/24:4)
				PE(O-16:0/20:5)
				PG(18:0/18:1)
				PG(O-18:1/24:1)
				PG(O-20:0/16:0)
				PG(O-20:0/18:2)
				PG(O-20:1/18:0)
				PG(O-20:1/22:1)
				PG(O-20:1/24:0)
				PG(O-22:1/16:0)
				PG(O-24:0/20:3)
				PG(O-24:1/16:0)
				PG(O-24:1/20:2)

				PG(P-20:1/16:0)
				PG(P-20:1/24:0)
				PG(P-24:1/16:0)
				PI(16:0/20:3)
				PI(16:1/18:0)
				PS(16:0/22:3)
				PS(18:0/22:3)
				PS(18:1/20:1)
				PS(18:1/22:2)
				PS(20:0/20:5)
				PS(22:0/16:3)
				PS(O-16:0/22:4)
				PS(O-18:0/20:2)
				PS(O-18:1/18:1)
				PS(O-18:1/22:5)
				PS(P-20:1/16:0)
				PS(P-20:1/20:2)
				PS(P-24:1/18:4)

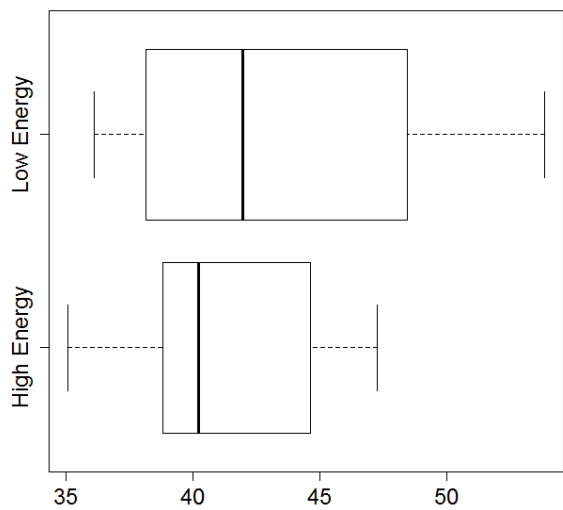


Figure S14. Pairwise overlap of phospholipid identifications for five replicates each of Low and High collision energy of human plasma data sets.

Table S16. Spectrum clusters versus Greazy identifications.

cluster id	species	spectra count
2210	PE(0:0/16:0)-H	4
2211	PE(0:0/16:0)-H	7
2212	PE(0:0/16:0)-H	1
3041	PE(0:0/18:2)-H	5
3042	PE(0:0/18:2)-H	1
3045	PE(0:0/18:2)-H	1
3068	PE(0:0/18:1)-H	1
3069	PE(0:0/18:1)-H	4
3070	PE(0:0/18:1)-H	1
3071	PE(0:0/18:1)-H	1
3101	PE(0:0/18:0)-H	1
3102	PE(0:0/18:0)-H	1
3114	PE(0:0/18:0)-H	1
3116	PE(0:0/18:0)-H	1
3118	PE(0:0/18:0)-H	20
3121	PE(0:0/18:0)-H	1
3123	PE(0:0/18:0)-H	3
3124	PE(0:0/18:0)-H	1
3126	PE(0:0/18:0)-H	1
3274	PE(0:0/20:4)-H	1
4416	PC(0:0/16:1)+CH3CO2	1
4421	PC(0:0/16:0)+CH3CO2	21
4730	PC(0:0/18:2)+CH3CO2	8
4732	PC(0:0/18:1)+CH3CO2	4
4753	PC(0:0/18:0)+CH3CO2	16
4916	PC(0:0/20:4)+CH3CO2	1
5757	PE(O-16:1/18:2)-H	7
5758	PE(O-16:1/18:2)-H	1
5849	PE(16:0/18:2)-H	5
5850	PE(16:0/18:2)-H	3
5852	PE(16:0/18:2)-H	1
5853	PE(16:0/18:1)-H	2
5879	PE(O-16:1/20:4)-H	15
5882	PE(O-16:1/20:3)-H	1
5884	PE(O-16:1/20:3)-H	1
5884	PE(P-18:1/18:2)-H	6
5886	PE(O-18:1/18:2)-H	4
5888	PE(O-18:1/18:1)-H	1
5949	PE(16:0/20:4)-H	1
5952	PE(16:0/20:4)-H	2
5990	PE(18:1/18:2)-H	5
6006	PE(18:0/18:2)-H	1
6007	PE(18:0/18:2)-H	2
6005	PE(18:0/18:2)-H	23
6005	PE(18:1/18:1)-H	1
6009	PE(18:0/18:1)-H	1
6038	PE(O-16:1/22:6)-H	7
6044	PA(O-18:0/18:1)+CH3CO2	1
6047	PA(O-18:0/18:1)+CH3CO2	1

6047	PA(O-20:1/16:0)+CH ₃ CO ₂	1
6062	PE(O-18:1/20:5)-H	1
6062	PE(P-18:1/20:4)-H	24
6063	PE(P-18:1/20:4)-H	1
6066	PE(O-18:1/20:4)-H	17
6133	PG(P-20:1/16:0)-H	1
6135	PG(P-20:1/16:0)-H	1
6164	PG(O-20:1/16:0)-H	4
6168	PE(16:0/22:6)-H	6
6207	PG(O-20:0/16:0)-H	1
6268	PE(18:1/20:4)-H	1
6271	PE(18:1/20:4)-H	1
6269	PE(18:0/20:5)-H	1
6281	PE(18:1/20:3)-H	2
6281	PE(18:0/20:4)-H	1
6282	PE(18:0/20:4)-H	22
6296	PA(P-24:1/14:0)+CH ₃ CO ₂	1
6307	PA(O-20:0/18:1)+CH ₃ CO ₂	1
6307	PG(18:0/18:1)-H	1
6304	PG(18:0/18:1)-H	1
6310	PS(O-20:0/16:0)-H	1
6373	PE(O-12:1/24:4)+CH ₃ CO ₂	1
6373	PE(O-16:0/20:5)+CH ₃ CO ₂	1
6375	PG(O-20:0/18:2)-H	1
6375	PG(O-22:0/16:2)-H	1
6375	PG(O-22:1/16:1)-H	3
6379	PC(14:0/18:2)+CH ₃ CO ₂	1
6387	PG(O-20:1/18:0)-H	2
6387	PG(O-22:1/16:0)-H	2
6390	PE(18:0/22:6)-H	1
6392	PC(14:0/18:1)+CH ₃ CO ₂	1
6392	PC(16:0/16:1)+CH ₃ CO ₂	2
6397	PC(16:0/16:0)+CH ₃ CO ₂	2
6461	PA(O-24:1/16:0)+CH ₃ CO ₂	1
6491	PC(16:0/18:3)+CH ₃ CO ₂	1
6491	PC(16:1/18:2)+CH ₃ CO ₂	2
6495	PG(O-22:1/18:1)-H	1
6495	PG(P-24:1/16:0)-H	1
6497	PC(16:0/18:2)+CH ₃ CO ₂	33
6497	PC(16:1/18:1)+CH ₃ CO ₂	2
6499	PG(O-24:1/16:0)-H	1
6511	PC(16:0/18:1)+CH ₃ CO ₂	42
6576	PS(O-14:0/22:2)+CH ₃ CO ₂	1
6576	PS(O-18:1/18:1)+CH ₃ CO ₂	1
6576	PS(P-20:1/16:0)+CH ₃ CO ₂	2
6580	PI(16:0/18:2)-H	23
6586	PI(16:0/18:1)-H	18
6586	PI(16:1/18:0)-H	1
6590	PC(16:0/20:5)+CH ₃ CO ₂	6
6595	PC(16:0/20:4)+CH ₃ CO ₂	24
6595	PC(16:1/20:3)+CH ₃ CO ₂	2

6601	PA(22:1/20:2)+CH ₃ CO ₂	1
6601	PA(24:1/18:2)+CH ₃ CO ₂	1
6603	PC(16:0/20:3)+CH ₃ CO ₂	17
6603	PC(18:1/18:2)+CH ₃ CO ₂	20
6610	PA(18:1/24:1)+CH ₃ CO ₂	1
6611	PG(O-18:1/24:1)-H	1
6611	PG(O-20:1/22:1)-H	1
6611	PG(O-24:0/18:2)-H	1
6612	PC(16:0/20:2)+CH ₃ CO ₂	3
6612	PC(18:0/18:2)+CH ₃ CO ₂	37
6612	PC(18:1/18:1)+CH ₃ CO ₂	1
6618	PG(O-20:1/22:0)-H	4
6651	PC(18:0/18:1)+CH ₃ CO ₂	17
6672	PC(P-16:1/22:5)+CH ₃ CO ₂	1
6672	PC(P-18:1/20:5)+CH ₃ CO ₂	1
6672	PS(P-18:1/24:4)-H	1
6672	PS(P-24:1/18:4)-H	1
6698	PS(O-16:0/22:4)+CH ₃ CO ₂	1
6698	PS(O-18:1/20:3)+CH ₃ CO ₂	1
6698	PS(O-24:0/14:4)+CH ₃ CO ₂	1
6716	PG(16:0/22:4)+CH ₃ CO ₂	1
6716	PI(16:0/20:4)-H	16
6726	PS(P-20:1/18:1)+CH ₃ CO ₂	3
6734	PI(16:0/20:3)-H	4
6734	PI(18:1/18:2)-H	6
6742	PS(O-18:0/20:2)+CH ₃ CO ₂	1
6745	PI(18:0/18:2)-H	26
6752	PI(18:0/18:1)-H	9
6771	PC(16:0/22:6)+CH ₃ CO ₂	3
6771	PC(18:1/20:5)+CH ₃ CO ₂	1
6772	PC(16:0/22:5)+CH ₃ CO ₂	9
6772	PC(18:1/20:4)+CH ₃ CO ₂	3
6777	PC(16:0/22:4)+CH ₃ CO ₂	1
6777	PC(18:0/20:4)+CH ₃ CO ₂	10
6778	PG(O-24:0/20:3)-H	1
6778	PG(O-24:1/20:2)-H	1
6784	PC(18:0/20:3)+CH ₃ CO ₂	22
6789	PG(O-24:1/20:1)-H	1
6789	PG(P-20:1/24:0)-H	2
6790	PS(16:0/22:3)+CH ₃ CO ₂	7
6790	PS(18:0/20:3)+CH ₃ CO ₂	4
6790	PS(22:0/16:3)+CH ₃ CO ₂	1
6790	PS(P-20:1/24:6)-H	2
6790	PS(P-24:1/20:6)-H	2
6813	PG(O-20:1/24:0)-H	2
6813	PG(O-24:0/20:1)-H	1
6817	PS(16:0/22:2)+CH ₃ CO ₂	1
6817	PS(18:1/20:1)+CH ₃ CO ₂	1
6817	PS(20:0/18:2)+CH ₃ CO ₂	1
6817	PS(P-24:1/20:5)-H	1
6821	PS(16:0/22:1)+CH ₃ CO ₂	1

6821	PS(18:0/20:1)+CH3CO2	2
6836	PS(O-18:1/22:5)+CH3CO2	1
6836	PS(P-20:1/20:4)+CH3CO2	1
6854	PI(18:1/20:4)-H	13
6864	PS(P-20:1/20:2)+CH3CO2	1
6867	PI(18:0/20:4)-H	36
6884	PI(18:0/20:3)-H	10
6909	PS(22:1/22:6)-H	1
6909	PS(24:1/20:6)-H	1
6932	PC(18:0/22:5)+CH3CO2	2
6959	PS(16:0/24:5)+CH3CO2	1
6965	PS(20:0/20:5)+CH3CO2	1
6983	PS(18:1/22:3)+CH3CO2	1
6993	PS(18:0/22:3)+CH3CO2	3
6993	PS(18:1/22:2)+CH3CO2	1
7055	PS(P-18:1/24:6)+CH3CO2	1

Table S17: Comparison of Fragment Counts - Greazy/LipidBlast (v49)/Common

	+H	+Na	-H (-2H)
PC	12/7/6	19/8/8	
Lyso-PC	8/4/3	12/2/1	
Plasmenyl-PC	8/5/3	8/4/4	
PE	10/8/7	19/4/4	17/6/6
Lyso-PE	6/5/3	12/4/2	10/4/3
Plasmenyl-PE	6/5/1	8/6/4	12/3/3
PS	10/6/5	20/4/4	16/7/7
PA		13/7/6	10/6/6
PI			22/8/8
PG			18/8/8
CL (-H)			42/15/15
CL (-2H)			34/12/10

Supplemental Text S4: Lipid precursors for which Greazy and LipidBlast both contain fragmentation models are represented in Table S17. Each entry provides the peak counts for models from both systems as well as the number of common peaks between the two (Greazy/LipidBlast (v49)/Common). There were a number of notable differences in fragment selection. The loss of water is a common fragment found among the LipidBlast models but largely absent in those from Greazy, the treatment of the vinyl-ether linked fatty acid differs between the two, and there are a number of small fragments in the Greazy models that represent the glycerol backbone. The smaller fragments that are out of an instruments scan range are not considered in Greazy's scoring algorithms. Both systems contain models for sphingomyelins but use different precursors. Greazy also contains models for Cer-PE, Cer-PI, and phosphoinositides while LipidBlast contains an additional 14 lipid classes not covered in Greazy. Another significant difference between the two systems is the inclusion of expected intensities in the LipidBlast models while Greazy incorporates intensities into the scores without any such inference. In Greazy the aim was to focus on a narrow set of lipids and to produce models that were as extensive as possible and let the probabilistic scoring algorithms sort out the correct identification. LipidBlast, as with many other systems, would seem to take a broader approach and focus on those key fragments that represent the constituent parts of a lipid.